Journal of Magnetism and Magnetic Materials 320 (2008) 2345–2349

Contents lists available at ScienceDirect

Journal of Magnetism and Magnetic Materials

journal homepage: www.elsevier.com/locate/jmmm

Tuning the band gap of self-assembled superparamagnetic photonic crystals in colloidal magnetic fluids using external magnetic fields

Shengli Pu [a,*], Tao Geng [a], Xianfeng Chen [b], Xianglong Zeng [c], Ming Liu [a], Ziyun Di [b]

[a] College of Science, University of Shanghai for Science and Technology, Shanghai 200093, China
[b] Department of Physics, The State Key Laboratory on Fiber Optic Local Area Communication Networks and Advanced Optical Communication Systems, Shanghai Jiao Tong University, Shanghai 200240, China
[c] Key Laboratory of Special Fiber Optics and Optical Access Networks, Ministry of Education, SCIE, Shanghai University, Shanghai 200072, China

ARTICLE INFO

Article history:
Received 9 March 2008
Available online 26 April 2008

PACS:
75.50.Mm
42.70.Qs
64.75.Yz
85.70.Sq

Keywords:
Magnetic fluid
Photonic crystal
Self-assembly

ABSTRACT

The model of tunable superparamagnetic photonic crystals self-assembled in colloidal magnetic fluids under externally applied magnetic fields is established. The mechanisms, which are in charge of the tunability of the band gaps with magnetic fields are clarified. The band structures of the triangularly-arrayed two-dimensional photonic crystals with limited heights of magnetic columns are calculated with the experimental data of structures and refractive indices in the literatures. The field-dependent properties of the first band gaps are gained for the *z*-odd and *z*-even modes, respectively. Simulation results indicate that the mid frequencies of the first band gaps of the *z*-odd modes can be easily tuned by the external magnetic fields, while those of the *z*-even modes bear relatively weak dependence on the external magnetic fields. Simultaneously, the first band gaps of both kinds of modes become wide along with the increase of the magnetic fields. The results presented in this work give a guideline for realizing the tunable photonic crystals with magnetically colloidal materials and magnetic stimuli.

1. Introduction

Structures of periodic variation of refractive index, known as photonic band gap materials or photonic crystals (PCs), may possess the property of prohibiting the transmission of a certain range of frequencies completely, which has been demonstrated both theoretically and confirmed experimentally [1,2]. The underlying concept of PCs was pioneered by Yablonovitch and John in 1987 [3,4]. Since then, PCs attract great interest due to their potential and versatile applications. With the development of design and fabrication of PCs, some fascinating features and applications of PCs have been presented, such as negative refraction [5–8], peculiar chromatic dispersion [9], superprisming effect [10,11]. Besides the conventional all-dielectric PCs, PCs made from metals [6], oxides [7,11,12] and magnetic materials [5,10,13–15] are also proposed and realized. These kinds of PCs can bear some unique properties over the conventional ones. Especially, the widths of the band gaps of the magnetic PCs are revealed to depend on the magnetic permeabilities of the magnetic materials, which is desirable for some applications [13,16].

On the other hand, microlithographic techniques and micromachining are the two main approaches for fabricating PCs in the past two decades. These methods are usually used to make PCs based on solid-state materials. Recently, self-assembly is employed to fabricate PCs in colloids [17–19] or binary-phase systems [20,21]. And the self-assembled PCs consisting of magnetic materials are advantageous due to their tunable photonic band gap by changing external magnetic fields [17,19–21]. The photonic-band-gap-tunable PCs are favorable for many pragmatic applications and hence get much attention from researchers and engineers [22,23]. Moreover, the on-line tunability can be realized by the magnetically self-assembled PCs, which excels other tunable PCs by changing the concentrations or ingredients of the constituent materials.

Magnetic fluids, as easily made and mature nanoscale magnetic materials, are colloidal systems of ultrafine magnetic nanoparticles dispersed in suitable liquid carriers [24]. Generally, they are superparamagnetic assigned to the small sizes of the single-domain magnetic particles. Accordingly, many practical applications based on the uniquely magnetic and colloidal features of magnetic fluids have been realized or are under intensive research [25–27]. In addition, the remarkable optical properties and late-model applications to photonic devices of colloidal magnetic fluids have been explored and proposed since the end of the 20th century [28–32]. Magnetic fluids, as optically

* Corresponding author. Tel.: +86 21 55274932; fax: +86 21 55270559.
E-mail address: shlpu@usst.edu.cn (S. Pu).

0304-8853/$ - see front matter © 2008 Elsevier B.V. All rights reserved.
doi:10.1016/j.jmmm.2008.04.134

functional materials in colloidal phase, are also excellent candidates for fabricating PCs, especially the band-gap-tunable PCs. This work focuses on the tunability of band gap of the PCs made from magnetic fluids via theoretical simulations utilizing the experimental data in the literatures. These results indicate that the magnetic fluids as alternative photonic band gap materials can actualize the tunable PCs in a different means (i.e. magnetic stimuli) and are desirable for potential photonic applications.

2. Model and mechanisms

Under externally magnetic fields, the magnetic nanoparticles within the magnetic fluids will agglomerate into columns or chains, which are contributed to the magnetism and then orderly arrangement of the particles along the magnetic fields. This phase separation and ordering structure formation of magnetic fluids under external magnetic fields have been studied extensively [33–36]. And it is unambiguous that magnetically periodic columns are formed in the magnetic fluids when the externally magnetic fields (perpendicular to the surfaces of the samples) are applied over certain critical values (usually tens of Oersteds) [36]. These periodic columns are usually in hexagonal pattern assigned to the condition of minimum total energy [37]. Therefore, this structural pattern is a kind of two-dimensional PC substantially. But the magnetic columns are of finite length because of the finite thickness of the samples in practice. So, strictly speaking, it is quasi-two-dimensional PC with periodic variation of refractive index in two dimensions and trilayer-slab-like structures in the third dimension. Herein, we call it as PC slab and its schematic is shown in Fig. 1.

The index contrast is a critical parameter to determine the band diagram of the PC, so knowing the information of refractive indices of the magnetic fluids with magnetic fields is vital. It is well-known that the magnetic fluids become two-phase systems (solid and liquid phases) when the external magnetic fields are beyond critical values. The solid phase is the magnetic columns (or chains) and the liquid phase is still the magnetic fluids but with decreasing concentration of magnetic nanoparticles. The dielectric constants of the magnetic columns are close to those of the used magnetic materials in solid state and do not vary with the external magnetic fields. However, the dielectric constant of the liquid phase decreases with the magnetic fields due to more magnetic nanoparticles aggregating into magnetic columns and then the reduction of concentration of the magnetic nanoparticles in the liquid phase at higher magnetic fields. With the theory of effective dielectric constant of two-phase system, the effective dielectric constant of the above PC slab ε_{PCS} is given by [38,39]

$$\varepsilon_{PCS} = \frac{-(\varepsilon_{col}-\varepsilon_{liq})(1-f)+\sqrt{[(\varepsilon_{col}-\varepsilon_{liq})(1-f)]^2+4\varepsilon_{col}\varepsilon_{liq}(1+f)^2}}{2(1+f)} \quad (1)$$

where ε_{col} and ε_{liq} are the dielectric constants of the magnetic columns (solid phase) and the liquid phase, respectively; $f=(A_{col}/A)/(1-A_{col}/A)$ and A_{col} is the area occupied by the magnetic columns within an area of A. The index contrast of the PC slab is related with ε_{col} and ε_{liq}. ε_{col} is a constant for a given magnetic material, e.g. $\varepsilon_{col}=n_{col}^2=2.2^2$ (n_{col} denotes the refractive indices of the magnetic columns) for Fe_3O_4 in the visible and near infrared ranges [40,41]. And ε_{liq} can be calculated from Eq. (1) for given values of ε_{PCS} and f, which can be expressed as

$$\varepsilon_{liq} = \frac{\varepsilon_{PCS}^2(1+f)+\varepsilon_{PCS}\varepsilon_{col}(1-f)}{\varepsilon_{PCS}(1-f)+\varepsilon_{col}(1+f)} \quad (2)$$

ε_{PCS} and f as functions of magnetic field strength can be obtained through experimental measurement [42,43] and from the micrographs taken at different strengths of magnetic field, respectively. In addition, the ratio of diameters d to periods a of the magnetic columns (namely d/a) also varies with the external magnetic field. Consequently, the band diagram of the PC slab can be influenced by the magnetic field, which may achieve the function of tunability.

In order to calculate the magnetic-field-dependent band diagram of the PC slab, we refer to a set of experimental data in a literature for a typical magnetic fluid sample (water-based magnetite magnetic fluid thin film with thickness $h=11.8\,\mu m$, volume fraction $\phi=1.52\%$, temperature $T=24.3\,^{\circ}C$, and sweep rate of magnetic field $dH/dt=10\,Oe/s$) [44]. Table 1 lists the original experimental data and the derived ones for the magnetic fluid sample at several discrete strengths of magnetic field. The PCs can only form within the magnetic fluids at strength of

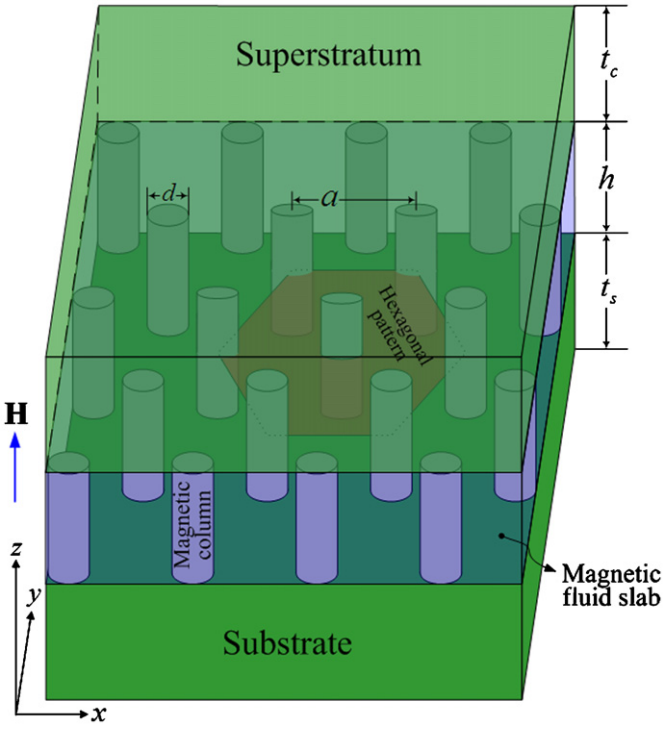

Fig. 1. Schematic of the PC slab formed in a magnetic fluid under externally perpendicular magnetic field and confined by the substrate and superstratum along the direction of magnetic field. a, d and h are the periods, diameters and heights of the magnetic columns, respectively.

Table 1
Refractive index n_{PCS} and area ratio A_{col}/A of the PC slab as functions of magnetic field [44]

H (Oe)	n_{PCS}	A_{col}/A	ε_{PCS}	f	d/a	ε_{liq}
75	1.4631	0.039	2.1407	0.0406	0.2074	2.0745
100	1.4637	0.063	2.1424	0.0672	0.2636	2.0339
125	1.4646	0.093	2.1451	0.1025	0.3202	1.9818
150	1.4655	0.124	2.1477	0.1416	0.3698	1.9255
175	1.4661	0.144	2.1494	0.1682	0.3985	1.8880
200	1.4664	0.157	2.1503	0.1862	0.4161	1.8628
225	1.4667	0.166	2.1512	0.1990	0.4278	1.8453
250	1.4669	0.172	2.1518	0.2077	0.4355	1.8335

The values of the relative parameters (ε_{PCS}, f, d/a, ε_{liq}) are calculated according to $\varepsilon_{PCS}=n_{pcs}^2$, $f=(A_{col}/A)/(1-A_{col}/A)$, $d/a=\sqrt{(2\sqrt{3}/\pi)(A_{col}/A)}$ and the theory of effective dielectric constant of two-phase system, respectively.

magnetic field higher than the critical value for the ordered formation (discriminating from disordered formation) of magnetic columns. This critical magnetic field somewhat depends on many parameters of the magnetic fluid sample and different magnetic fluids and is usually around tens of Oersteds. Without loss of generality, the lowest strength of magnetic field is selected at 75 Oe herein. For the specific cases, the critical magnetic field may be slightly larger or smaller than 75 Oe. And then, it is much more appropriate to take the values of field strength in this work as relative ones rather than the actual values. The values of n_{PCS} (refractive index of the PC slab) and A_{col}/A in Table 1 are extracted from Ref. [44] directly. The values of ε_{PCS} are calculated according to $\varepsilon_{PCS} = n_{PCS}^2$ (the magnetic permeability of the PC slab is taken as 1 [45] because the forbidden band is mostly in the range of infrared ranges due to the scale of the period of the magnetic columns in several micrometers [35]). The values of f and ε_{liq} are attained via $f = (A_{col}/A)/(1-A_{col}/A)$ and Eq. (2), respectively. For hexagonal structural patterns as shown in Fig. 1, $A_{col}/A = \pi d^2/(2\sqrt{3a^2})$. Consequently, the values of d/a can be calculated through $d/a = \sqrt{(2\sqrt{3}/\pi)(A_{col}/A)}$.

It is evident from Table 1 that ε_{liq} decreases with magnetic field. As a result, the indices contrast between the magnetic columns and the liquid phase, defined as $\delta = n_{col} - n_{liq} = 2.2 - \sqrt{\varepsilon_{liq}}$ (where n_{liq} is the refractive index of the liquid phase), increases with magnetic field. At the same time, d/a increases with the magnetic field as well. These two factors are crucial to the structures of the band diagram of the PC slab.

3. Simulation results and discussion

In the case of PC slab as shown in Fig. 1, the light propagates in the xy-plane and is confined in the z-direction by index guiding. That is, all the guiding modes in the PC slab should have effective refractive indices larger than the refractive index of the substrate and the superstratum according to the theory of waveguide optics. On the contrary, the effective refractive indices of the radiation modes are smaller than the refractive index of the substrate or the superstratum. We will only calculate the meaningful guiding modes in the band diagram. For the convenience of calculation, it is proper to consider the PC slab as a three-dimensionally periodic configuration. If the separation (in the z-direction) between two neighboring PC slab is sufficiently large, the coupling between them is negligible. In consequence, each PC slab can be regarded as an independent one and then the simulation results converge to those of the actual structure. The ratio of the height h to the separation a of the magnetic columns increases with the magnetic field and is generally in the range of 1–4 according to the experimental evidence [35]. In the following calculation, we firstly fix the value of h/a at 2 and set the period of the PC slab in the z-direction as $8a$. So the separation between the adjacent PC slabs is large enough and the correct results are acquired. The effect of the magnetic-field-dependent h/a will be qualitatively discussed late. Without loss of generality, the refractive indices of the substrate (n_s) and the superstratum (n_s) are assumed to be the same value and be equal to that of the liquid phase, viz. $n_{liq} = n_{s=} n_c$.

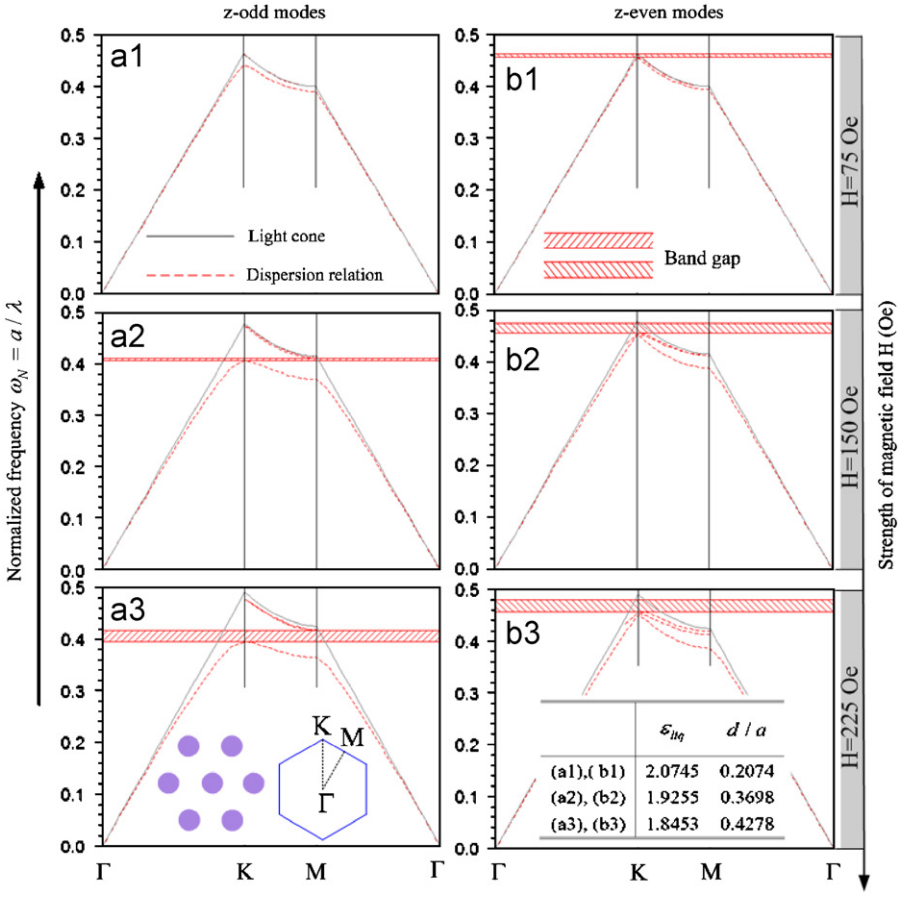

Fig. 2. Band diagrams for (a) z-odd and (b) z-even modes at three discrete strengths of magnetic field: (1) 75, (2) 150 and (3) 225 Oe. The solid lines indicate the light cone. The dashed lines and the shaded regions are the dispersion curves and the band gaps, respectively. The low left inset shows the structure of triangularly-arrayed PC and the first Brillouin zone in the wave-vector space. The low right inset tabulates the critical parameters for the band diagrams calculation.

The photonic band structures of the guided modes propagating in the PC slab shown in Fig. 1 can be calculated using the standard plane-wave expansion method. The typical band diagrams for *z*-odd and *z*-even modes at three different strengths of magnetic field are plotted in Fig. 2(a) and (b), respectively. The ordinate in Fig. 2 denotes frequency, which has been normalized to $2\pi c/a$ (c is the light speed in vacuum) and equals a/λ, i.e. $\omega_N = a/\lambda$. The solid lines indicate the light cone and only the guided modes below this line have been plotted. All of the radiation modes are above the light cone and abandoned in Fig. 2 owing to their meaninglessness. The dashed lines in Fig. 2 are the corresponding bands of the guiding modes in the PC slab and the shaded regions are the band gaps. It is obvious from Fig. 2(a) that the forbidden band of the *z*-odd modes only exists at high magnetic field. Nevertheless, the forbidden band of the *z*-even modes always exists in the same range of magnetic field as displayed in Fig. 2(b). Another interesting finding is that the widths of the first band gaps of the *z*-odd modes as well as the *z*-even modes increase with the magnetic field. However, their positions in the band diagrams shift into opposite directions with magnetic field for different kinds of guided modes (*z*-odd or *z*-even).

To distinctly understand the magnetic-field-dependent band gaps of the PC slab, the band structures at different strengths of magnetic field are calculated with the data listed in Table 1. Then, the widths and positions of the first band gaps are achieved and plotted in Fig. 3(a) and (b) for *z*-odd and *z*-even modes, respectively. The solid symbols denote the middle of the band gaps and the vertical bars mark the spans of the band gaps. Fig. 3 explicitly depicts the aforementioned properties of the first band gaps with magnetic field. Strictly, the gap ratio defined as the width of the full gap to the mid-frequency of the gap is more suitable to characterize the band size of the forbidden band. The ratios of the first band gaps as functions of magnetic field are figured and plotted in Fig. 3 as hollow symbols and dashed lines. Similar to the widths of the band gaps, the gap ratios increase with the external magnetic field for both kinds of modes as shown in Fig. 3.

In the above calculations, we have simply fixed the value of h/a at 2 for different magnetic fields. Accurately, h/a increases slightly with magnetic field due to the reduction of the period a of the magnetic columns, although the thickness of the sample h (or the height of the magnetic columns) is invariable. To consider the thickness-dependent effect of the band gaps, we have recalculated the band structures of the PC slab at several reasonable values of h/a for definite strengths of magnetic field and the thickness-dependent properties of the forbidden bands are attained. Extensive calculation manifest that almost the same trend of change of the first forbidden band gaps with thickness h/a of the PC slab happens for different strengths of magnetic field, although this may not be the universal rule. A typical example is shown in Fig. 4 for magnetic field strength of 175 Oe. Fig. 4(a) reveals that the band gap of the *z*-odd modes shifts to low frequency and a maximum width of the band gap occurs for certain value of the thickness of PC slab. This result coincides with that reported by Hong et al. [16]. Fig. 4(b) presents the analogous tendency for the *z*-even modes as the *z*-odd modes shown in Fig. 4(a).

Taking the practical situation into account, the mid-frequency of the first band gap of the *z*-odd modes ought to have a deeper dependence on the magnetic field than that shown in Fig. 3(a) due to the increase of the value of h/a (assigned to the reduction of the

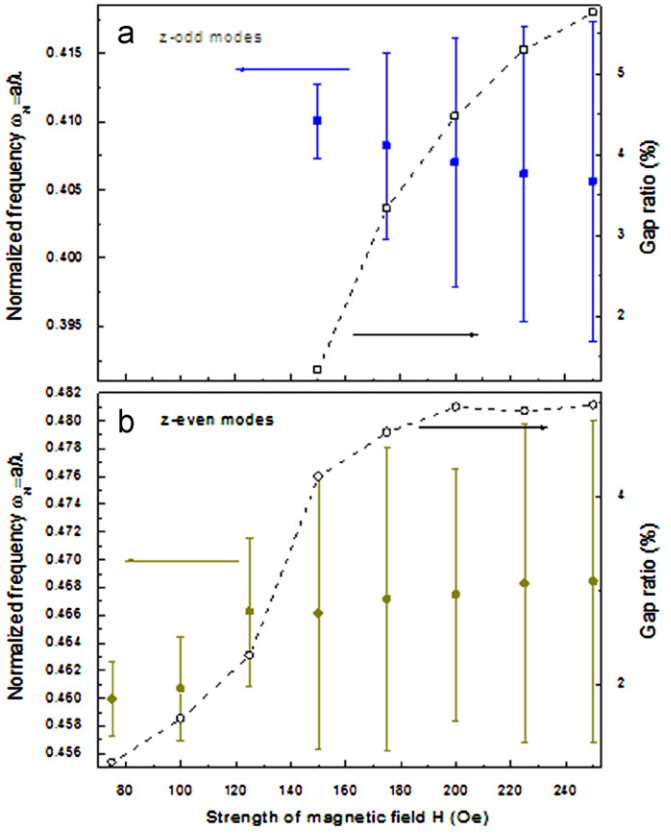

Fig. 3. The first band gaps of (a) *z*-odd and (b) *z*-even modes as functions of magnetic field. The solid symbols denote the middle of the band gaps and the vertical bars mark the spans of the band gaps. The hollow symbols and dashed lines (guided to the eyes) correspond to the gap ratios of the first band gaps.

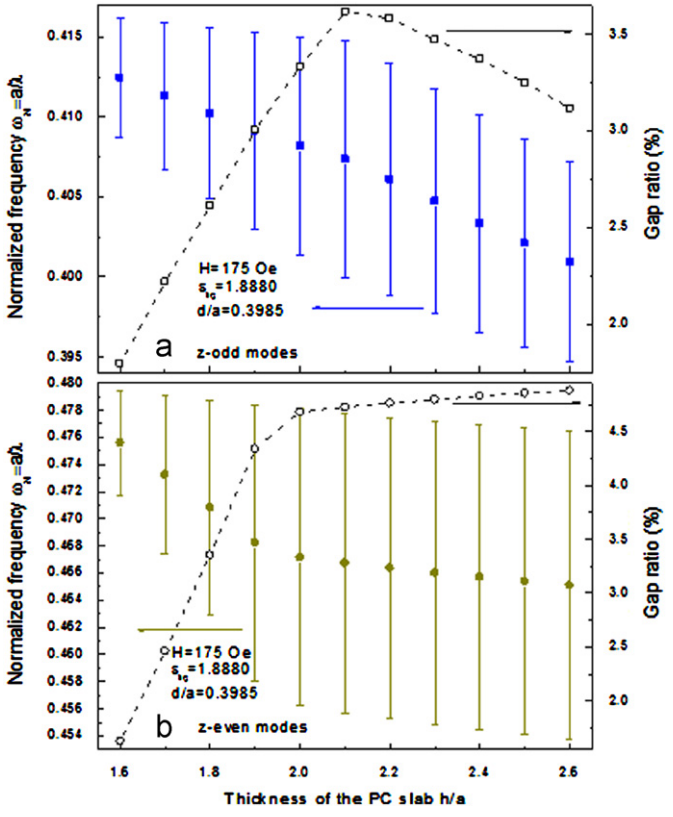

Fig. 4. The first band gaps of (a) *z*-odd and (b) *z*-even modes as functions of thickness h/a of the PC slab at fixed strength of magnetic field (175 Oe). The solid symbols denote the middle of the band gaps and the vertical bars mark the spans of the band gaps. The hollow symbols and dashed lines (guided to the eyes) correspond to the gap ratios of the first gaps.

value of a in nature) according to Fig. 4(a). This will result in the large tunability with magnetic field and is favorable for practical applications. But the thickness-dependent band gap of the z-even modes shown in Fig. 4(b) will counteract their tunability with magnetic field shown in Fig. 3(b) more or less. As a result, the mid-frequency of this kind of band gap is weakly dependent on magnetic field. On the whole, the widths of the first band gaps of both kinds of modes always increase with magnetic field in the light of Figs. 3 and 4. It is worth noting that this post-thickness-modification process is unnecessary if the actual thickness of the sample h is far lager than the period a or the exact values of a at different magnetic fields are known. In these two cases, the relative thickness of the PC slab h/a can be considered as a constant at all magnetic fields or the exact values of h/a for different magnetic fields can be implemented for precise band structures calculation.

Finally, we would like to point out that Yang et al. [46] have experimentally confirmed the magnetic-field-induced tunability of the band gap of the PC slab self-assembled in the $MnFe_2O_4$ magnetic fluid lately. And Ge et al. [17] have also demonstrated the highly tunable superparamagnetic colloidal photonic crystals by magnetic-field-induced self-assembly with tunable range across the entire visible spectrum and rapid optical response. All of these convince us of the promising future and potentially valuable applications of self-assembled superparamagnetic photonic crystals with magnetic materials. However, a vital factor may hamper the advancement of applications of this kind of tunable PCs is the relatively strong absorption of magnetic materials at optical frequencies. Delightfully, many researchers are working on this issue and trying to overcome the problem. At present, the highly transparent magnetic nanocomposites and magnetic fluid in optical frequencies have been fabricated by several authors [47–52]. We are now embarking on synthesizing and fabricating the optically transparent magnetic nanostructured materials in collaboration with researchers in chemistry and nanoscience. In a word, the prospects of the self-assembled superparamagnetic PCs are observable in view of the theoretical predications in this work and the development of material science.

4. Conclusions

In conclusion, the magnetic-field-dependent refractive indices of the liquid phase (or the index contrast between the liquid phase and solid one) and periods of the magnetic columns are crucial to the tunability of the band gaps of the PC slab with magnetic fields. Comparing with z-even modes, operating at z-odd modes is more appropriate for shifting the mid frequencies of the first band gaps to the desired positions in the reasonable range. This tunable feature is the basic concept of tunable filter in optics and may be exploited to make the corresponding tunable photonic devices. Another unique point is the enhancement of the widths of the first band gaps with magnetic fields for both kinds of guided modes. This property might be used to develop tunable attenuator for optical communication. But actualization of these prototypes need further detailed investigation and development of correlative science.

Acknowledgments

This research is supported by the National Natural Science Foundation of China (No. 10704048); the Research Fund for Selecting and Training Excellent Young Teachers in Universities of Shanghai, Shanghai Municipal Education Commission (No. 563804); the Scientific Research Initiative Fund for the Doctorates in University of Shanghai for Science and Technology (No. X729); and the National Basic Research Program "973" of China (No. 2007CB307000).

References

[1] J.D. Joannopoulos, R.D. Meade, J.N. Winn, Photonic Crystals, Princeton University Press, Princeton, NJ, 1995.
[2] J.D. Joannopoulos, P.R. Villeneuve, S. Fan, Nature (London) 386 (1997) 143.
[3] E. Yablonovitch, Phys. Rev. Lett. 58 (1987) 2059.
[4] S. John, Phys. Rev. Lett. 58 (1987) 2486.
[5] S.Y. Yang, C.-Y. Hong, H.C. Yang, J. Opt. Soc. Am. A 23 (2006) 956.
[6] P.V. Parimi, W.T. Lu, P. Vodo, J. Sokoloff, J.S. Derov, S. Sridhar, Phys. Rev. Lett. 92 (2004) 127401.
[7] E. Cubukcu, K. Aydin, E. Ozbay, S. Foteinopoulou, C.M. Soukoulis, Nature (London) 423 (2003) 604.
[8] M. Notomi, Opt. Quantum Electron. 34 (2002) 133.
[9] S.Y. Yang, C.T. Chang, J. Appl. Phys. 98 (2005) 023108.
[10] S.Y. Yang, C.T. Chang, J. Appl. Phys. 100 (2006) 083105.
[11] H. Kosaka, T. Kawashima, A. Tomita, M. Notomi, T. Tamamura, T. Sato, S. Kawakami, Phys. Rev. B 58 (1998) R10096.
[12] S.Y. Yang, P.H. Yang, C.D. Liao, J.J. Chieh, Y.P. Chen, H.E. Horng, C.-Y. Hong, H.C. Yang, Appl. Phys. Lett. 89 (2006) 231108.
[13] S.Y. Yang, C.-Y. Hong, I. Drikis, H.E. Horng, H.C. Yang, J. Opt. Soc. Am. B 21 (2004) 413.
[14] A. Saib, D.V. Janvier, I. Huynen, A. Encinas, L. Piraus, E. Ferain, R. Legras, Appl. Phys. Lett. 83 (2003) 2378.
[15] I.L. Lyubchanskii, N.N. Dadoenkova, M.I. Lyubchanskii, E.A. Shapovalov, T. Rasing, J. Phys. D: Appl. Phys. 36 (2003) R277.
[16] C.-Y. Hong, I. Drikis, S.Y. Yang, H.E. Horng, H.C. Yang, J. Appl. Phys. 94 (2003) 2188.
[17] J. Ge, Y. Hu, Y. Yin, Angew. Chem. Int. Ed. 46 (2007) 7428.
[18] F. Schüth, F. Marlow, Nature (London) 449 (2007) 550.
[19] X. Xu, G. Friedman, K.D. Humfeld, S.A. Majetich, S.A. Asher, Adv. Mater 13 (2001) 1681.
[20] Y. Saado, M. Golosovsky, D. Davidov, A. Frenkel, Phys. Rev. B 66 (2002) 195108.
[21] M. Golosovsky, Y. Saado, D. Davidov, Appl. Phys. Lett. 75 (1999) 4168.
[22] A.C. Arsenault, D.P. Puzzo, I. Manners, G.A. Ozin, Nat. Photonics 1 (2007) 468.
[23] Y.J. Liu, X.W. Sun, Jpn. J. Appl. Phys. 46 (2007) 6634.
[24] R.E. Rosensweig, Ferrohydrodynamics, Cambridge University Press, Cambridge, 1985.
[25] D. Brousseau, E.F. Borra, H.J. Ruel, J. Parent, Opt. Express 14 (2006) 11486.
[26] Y. Melikhov, S.J. Lee, D.C. Jiles, D.H. Schmidt, M.D. Porter, R. Shinar, J. Appl. Phys. 93 (2003) 8438.
[27] T. Neuberger, B. Schöpf, H. Hofmann, M. Hofmann, B.V. Rechenberg, J. Magn. Magn. Mater 293 (2005) 483 (and references therein).
[28] J.J. Chieh, S.Y. Yang, H.E. Horng, C.-Y. Hong, H.C. Yang, Appl. Phys. Lett. 90 (2007) 133505.
[29] S. Pu, X. Chen, Y. Chen, Y. Xu, W. Liao, L. Chen, Y. Xia, J. Appl. Phys. 99 (2006) 093516.
[30] S. Pu, X. Chen, L. Chen, W. Liao, Y. Chen, Y. Xia, Appl. Phys. Lett. 87 (2005) 021901.
[31] H.E. Horng, J.J. Chieh, Y.H. Chao, S.Y. Yang, C.-Y. Hong, H.C. Yang, Opt. Lett. 30 (2005) 543.
[32] S. Pu, X. Chen, W. Liao, L. Chen, Y. Chen, Y. Xia, J. Appl. Phys. 96 (2004) 5930.
[33] C.C. Shih, Y.S. Lin, C.Y. Wang, I.M. Jiang, M.S. Tsai, C.C. Ting, H.E. Horng, J. Magn. Magn. Mater 300 (2006) 306.
[34] S.Y. Yang, Y.H. Chao, H.E. Horng, C.-Y. Hong, H.C. Yang, J. Appl. Phys. 97 (2005) 093907.
[35] S.Y. Yang, H.E. Horng, C.-Y. Hong, H.C. Yang, M.C. Chou, C.T. Pan, Y.H. Chao, J. Appl. Phys. 93 (2003) 3457.
[36] C.-Y. Hong, H.E. Horng, F.C. Kuo, S.Y. Yang, H.C. Yang, J.M. Wu, Appl. Phys. Lett. 75 (1999) 2196.
[37] W. Wen, L. Zhang, P. Sheng, Phys. Rev. Lett. 85 (2000) 5464.
[38] D.A.G. Bruggeman, Ann. Phys. (Leipzig) 24 (1935) 636.
[39] S.Y. Yang, J.J. Chieh, H.E. Horng, C.-Y. Hong, H.C. Yang, Appl. Phys. Lett. 84 (2004) 5204.
[40] U. Buchenau, I. Müller, Solid State Commun. 11 (1972) 1291.
[41] P.C. Scholten, IEEE Trans. Magn. MAG-16 (1980) 221.
[42] S.Y. Yang, Y.F. Chen, H.E. Horng, C.-Y. Hong, W.S. Tse, H.C. Yang, Appl. Phys. Lett. 81 (2002) 4931.
[43] S. Pu, X. Chen, Y. Chen, W. Liao, L. Chen, Y. Xia, Appl. Phys. Lett. 86 (2005) 171904.
[44] H.E. Horng, C.-Y. Hong, S.Y. Yang, H.C. Yang, Appl. Phys. Lett. 82 (2003) 2434.
[45] L.D. Landau, E.M. Lifshitz, L.P. Pitaevskii, Electrodynamics of Continuous Media, Pergamon, London, 1984.
[46] S.Y. Yang, H.E. Horng, Y.T. Shiao, C.-Y. Hong, H.C. Yang, J. Magn. Magn. Mater 307 (2006) 43.
[47] S. Thomas, D. Sakthikumar, P.A. Joy, Y. Yoshida, M.R. Anantharaman, Nanotechnology 17 (2006) 5565.
[48] J.G. Moore, E.J. Lochner, C. Ramsey, N.S. Dalal, A.E. Stiegman, Angew. Chem. 115 (2003) 2847.
[49] M. Zayat, F.D. Monte, Adv. Mater 15 (2003) 1809.
[50] B.H. Sohn, R.E. Cohen, Chem. Mater 9 (1997) 264.
[51] R.F. Ziolo, E.P. Giannelis, B.A. Weinstein, M.P. O'Horo, B.N. Ganguly, V. Mehrotra, M.W. Russell, D.R. Huffman, Science 257 (1992) 219.
[52] A.F. Bakuzis, K.S. Neto, P.P. Gravina, L.C. Figueiredo, P.C. Morais, L.P. Silva, R.B. Azevedo, O. Silva, Appl. Phys. Lett. 84 (2004) 2355.